

# LIGHT SCATTERING OF NORMAL HUMAN LENS I

## APPLICATION OF RANDOM DENSITY AND ORIENTATION FLUCTUATION THEORY

FREDERICK A. BETTELHEIM AND MILAN PAUNOVIC, *Chemistry Department, Adelphi University, Garden City, New York 11530 U.S.A.*

**ABSTRACT** Light-scattering intensities in the  $I_{\parallel}$  and  $I_{+}$  mode were obtained on thin sections of three human lenses. Random density and orientation fluctuation theory, without cross correlation, was employed to evaluate light-scattering parameters. Both the density correlation distances, as well as the orientation correlation distances, were related to structural elements in the lens fiber cell that have been observed by other investigators with different techniques. The magnitude of these fluctuations were evaluated, and it was demonstrated that the density fluctuations are the main contributors to light scattering in normal human lenses. Changes in the light-scattering parameters were evaluated as a function of position within the lens. The changes observed agree with the biochemical data in the literature that reflects that an aging process occurs when one proceeds from the periphery of the lens toward the center.

### INTRODUCTION

The transparency of the lens has been explained by the absence of large fluctuations in the refractive index due to the relatively even protein distribution within the lens fibers (Trokkel, 1962; Philipson, 1973), and also by the size of the spatial Fourier components that are smaller than the wavelength of the light (Benedek, 1971). When both the size and the amplitude of the refractive index fluctuations increase, opacity will develop and provide the physical basis of cataract formation. Even in noncataractous lens the light scattering not only reduces the intensity of the light, but also causes glare and distortion of the image formation in the retina.

In a normal lens, most of the scattering comes from the fiber cell membranes that have higher refractive index than the surrounding cytoplasm. When fiber cells are regularly packed, the scattering gives rise to a diffraction pattern (Bettelheim and Vinciguerra, 1971; Bettelheim et al., 1973; Philipson, 1973). It has been suggested that such light scattering causes the halo around bright objects.

The light scattering of a normal lens is due to density fluctuation, since only the  $I_{\parallel}$  component of the polarized light yields diffraction patterns and the  $I_{+}$  component is absent. Thin membranes embedded in a medium of a different refractive index give rise to form birefringence and, therefore, besides density fluctuation, optical anisotropy fluctuation should also contribute to the refractive index fluctuation. Therefore, an  $I_{+}$  component should be observable. The absence of  $I_{+}$  component was explained by the balance between two components of the birefringence: form and intrinsic, canceling each other and eliminating the optical anisotropy fluctuation (Bettelheim, 1975, 1978). Cytoplasmic filaments, microfibrils,

etc., observed by a number of investigators (Wanko and Gavin, 1959; Lasser and Balazs, 1972; Maisel and Perry, 1972; Rafferty and Esson, 1974; Perry, 1976; Maisel, 1977; Rafferty and Goossens, 1978) may provide the optically anisotropic structures that are necessary for the presence of intrinsic birefringence. An upset of the birefringence balance, for example, during initial cataract formation, gives an  $I_+$  scattering component as was shown in galactose (Bettelheim, 1978) and xylose cataract formation (Bettelheim and Bettelheim, 1978).

The amount of light scattered by normal human lens is less than 5%. Above and beyond the diffraction-type scattering, the rest of the scattering is isotropic. The intensity of scattered light decreases monotonically with scattering angle,  $\theta$ , and is independent of the azimuthal angle. Such scattering is expected from random fluctuations in the refractive index. The purpose of this study is to apply the theory of random fluctuations in density as well in optical anisotropy, to analyze the angular distribution of scattering intensity of lens slices, and to obtain parameters that will describe the scattering units within the lens fibers.

### THEORY

Photons passing through an opaque medium encounter refractive index fluctuations and, therefore, will be scattered in all directions. The nature and magnitude of the scattering will depend on the structural elements causing the fluctuations, and conversely one can use the angular dependence of the scattered light intensity to elucidate the structures responsible for the fluctuations.

There are two kinds of fluctuations that can cause light scattering: density fluctuations; and fluctuations in the orientation of optically anisotropic material. Both will result in variation of the local refractive index as the photon is passing through the material (Fig.1).

In Fig. 1, the solid, straight line represents the average polarizability (refractive index) of the medium. The  $\eta$  shows the local deviation from this average and  $\bar{\eta}^2$  is the average (mean) squared deviation from the average refractive index. "a" is the size of the regions that are correlated.

The above symbols are used in the designation of density fluctuations. Similar symbols,  $\bar{\delta}^2$  and "b," are used in designating the orientation fluctuations. The reason for using two different designations for refractive index fluctuations is that in most cases one can separate the contributions coming from the two fluctuations. This is done by using plane polarized light as a light-source. If the scattering sample is placed between two polarizers whose axes of polarization are parallel, the measured scattered light intensity is designated as  $I_1$ . On the other hand, if the polarizer and analyzer are set  $90^\circ$  apart, the scattered light intensity is measured in the  $I_+$  mode.

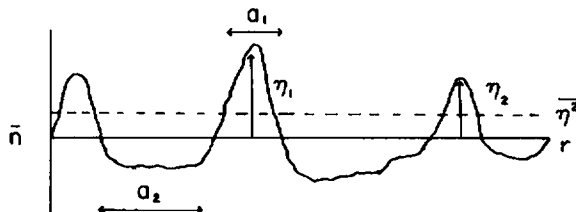


FIGURE 1 Fluctuations in refractive index as a function of distance ( $r$ ) in the scattering medium.

The theory of light scattering from random density and random orientation fluctuation (Stein et. al., 1959) predicts that

$$I_{\parallel} = K \left\{ \bar{\eta}^2 \int \gamma(r) \frac{\sin hr}{hr} r^2 dr + \frac{4}{45} \bar{\delta}^2 \int f(r) \left[ \frac{\bar{\eta}^2}{\alpha^2} \gamma(r) + 1 \right] \frac{\sin hr}{hr} r^2 dr \right\}; \quad (1)$$

$$I_{+} = K \left\{ \frac{1}{15} \bar{\delta}^2 \int f(r) \left[ \frac{\bar{\eta}^2}{\alpha^2} \gamma(r) + 1 \right] \frac{\sin hr}{hr} r^2 dr \right\}. \quad (2)$$

$\bar{\eta}^2$  and  $\bar{\delta}^2$  of Eqs. 1 and 2 are the average deviations in density and orientation fluctuations, respectively;  $h = (4\pi/\lambda) \sin (\theta/2)$  is a function of the scattering angle,  $\theta$ , where  $\lambda$  is the wavelength of the light in the medium;  $\alpha$  is the average polarizability of the sample, and  $r$  is the distance of penetration of light in the medium. The form of the correlation function is:

$$\gamma(r) = (\langle \eta_1 \eta_2 \rangle_r / \bar{\eta}^2). \quad (3)$$

For all pairs of volume elements separated by an  $r$  distance,  $\langle \eta_1 \eta_2 \rangle$  is the average of  $\eta_1 \eta_2$ ;  $\eta_1$  and  $\eta_2$  are, on the other hand, the local deviations (of refractive indices from the average) of two volume elements, separated by an  $r$  distance. The boundary conditions of the correlation function are:  $r = 0$ ,  $\gamma(0) = 1$ . When the two volume elements are the same, their separation is zero; perfect correlation exists. The other boundary condition is when the two volume elements are separated at  $r = \infty$ , no correlation exists and  $\gamma(\infty) = 0$ . Similarly the orientation correlation function,  $f(r)$ , obeys the same boundary conditions

$$f(r) = (\langle \delta_1 \delta_2 \rangle_r / \bar{\delta}^2), \quad (4)$$

namely when  $r = 0$ ,  $f(0) = 1$  and when  $r = \infty$ ,  $f(\infty) = 0$ . When only density fluctuations contribute to the light scattering,  $\bar{\delta}^2 = 0$ , Eq. 2 becomes zero, and there will be no  $I_{+}$  component of the light scattering. Under those conditions Eq. 1 reduces to the form given by Debye and Bueche (1949). When only orientation fluctuations cause light scattering,  $\bar{\eta}^2 = 0$ , and consequently the  $I_{\parallel}/I_{+}$  ratio should be 4/3.

If both density and orientation fluctuations contribute to the light scattering, as is the case in human lenses, Eqs. 1 and 2 must be solved analytically to obtain parameters describing the scattering units. The first step in this process is to be able to evaluate the nature of the correlation functions  $\gamma(r)$  and  $f(r)$ .

When four-thirds of  $I_{+}$  is subtracted from  $I_{\parallel}$ , Eqs. 1 and 2 give

$$\left( I_{\parallel} - \frac{4}{3} I_{+} \right) = K \bar{\eta}^2 \int \gamma(r) \frac{\sin hr}{hr} r^2 dr. \quad (5)$$

Using Fourier inversion one obtains

$$\gamma(r) = \frac{c}{r} \int_0^{\infty} \left[ I_{\parallel} - \frac{4}{3} I_{+} \right] h \sin hr dh. \quad (6)$$

The normalization constant,  $c$ , is chosen so that when  $r = 0$ ,  $\gamma(r) = 1$ .

Once the  $\gamma(r)$ , the density correlation function, is obtained, Eq. 5 can be used to calculate  $\bar{\eta}^2$ , the mean squared average deviation.

All the quantities in Eq. 5 are known, and if the  $I_{\parallel}$  and  $I_{+}$  intensities are given in Rayleigh ratios [ $R(\theta) = (I(\theta)/I(0))d^2$ ], the constant in Eq. 5 is

$$K = (4\Pi^2/\lambda_0^4), \quad (7)$$

where  $\lambda_0$  is the wavelength in vacuum and  $d$  is the distance between the sample and the photometer. Thus from the intensities (Rayleigh ratios) of  $I_{\parallel}$  and  $I_{+}$  at a set angle (set  $h$ ), the  $\bar{\eta}^2$  values can be calculated.

The experimental  $\gamma(r)$  can be obtained by the numerical integration of Eq. 6. The experimental  $\gamma(r)$  must be fitted to an analytical function obeying the boundary conditions.

In some cases (Debye and Bueche, 1949; Gallagher and Bettelheim, 1962) a single exponential function,

$$\gamma(r) = e^{-r/a}, \quad (8)$$

fitted the experimental density correlation function, where  $a$  was the correlation length of the density fluctuation.

In other experiments it was found (Stein, 1969; Wun and Prins, 1974) that the scattering over the entire angular range could be described by a sum of Gaussians,

$$\gamma(r) = \sum X_i e^{-(r^2/a_i^2)}, \quad (9)$$

where  $\sum X_i = 1$ .

To interpret such an experimental correlation function, one can consider the inhomogeneous system as a quasi two-phase system (dispersed and dispersant,  $i = 2$ .) Thus, two different correlation lengths would measure the size of inhomogeneities under those conditions:  $a_1$  and  $a_2$  are the average size of the dispersed and the dispersant phase, respectively (Kahovec et al., 1953; Kratky, 1966; Alexander, 1969).

When the proper analytical form of the experimental  $\gamma(r)$  is obtained, the  $\bar{\eta}^2$  values can be evaluated from Eq. 5 by using the Rayleigh ratio of intensities at a set angle.

Once this has been accomplished, the nature of the orientation correlation function  $f(r)$  can be obtained.

By using a new definition,

$$\mu(r) = 1 + (\bar{\eta}^2/\alpha^2)\gamma(r), \quad (10)$$

Eq. 2 takes the form

$$I_{+} = (1/15)K\bar{\delta}^2 \int f(r)\mu(r)(\sin hr/hr)r^2 dr. \quad (11)$$

The only unknown quantity in Eq. 10 is  $\alpha$ , the average polarizability, which can be obtained from the Lorentz-Lorenz equation, i.e., from the average refractive index,  $n$ , and average density,  $\rho$ , of the lens section

$$[(n^2 - 1)/(n^2 + 2)](1/\rho) = (4/3)\Pi\alpha. \quad (12)$$

The Fourier transform of Eq. 11 yields

$$f(r)\mu(r) = \frac{c}{r} \int_{h=0}^{\infty} I_{+} h \sin hr dh, \quad (13)$$

and thus the experimental orientation correlation function  $f(r)$  can be obtained. The experimental orientation correlation function can be expressed as the result of two kinds of

inhomogeneities and, similar to Eq. 9, the corresponding form of  $f(r)$  will be

$$f(r) = \sum X_i e^{-r^2/b_i^2}, \quad (14)$$

where  $i = 2$ .

With the aid of the analytical form of  $f(r)$ , Eq. 11 is rearranged and solved for  $\bar{\delta}^2$  at a set scattering angle.

## EXPERIMENTAL

Human lenses were obtained from the New York Eye Bank. Three sets of eyes were used. These were donated by patients: a 31-yr-old male, who died of metastatic colon cancer; a 59-yr-old male, who died of myocardial infarction; and an 82-yr-old male, who died of pneumonia. Enucleation of the eye occurred between 1 and 5 h after death, and the lens was used for light-scattering studies within 20 h post mortem. All lenses were clear, with no apparent cataract present.

Since the purpose of the experiment was to apply the theory of random fluctuations to the angular distribution of the intensities of the isotropic light scattering pattern, we wanted to avoid the diffraction type of scattering originating from the repeating distance provided by the regular packing of the fiber cells within the lens. Therefore, we wanted to study the light scattering of thin lens sections, 10  $\mu\text{m}$ , which is about the width of a fiber cell. Furthermore, the analysis of light-scattering pattern from thin sections reduced the problem of secondary and multiple scattering.

Thin sections of human lens were cut by a refrigerated microtome. The lenses were set on a planchet and precooled to  $-10$  and  $-20^\circ\text{C}$ . Sectioning was done from the anterior of the lens to the posterior perpendicular to the visual axis. Only sections that provided the cleanest cuts without crumbling, holes, etc., were retained. 10 such sections were used for light-scattering studies. The 10 best sections were retained for light-scattering studies and the rest were discarded. We noted the actual location of each section in millimeter distance from the anterior or posterior surface of the lens. Each lens section was taken up between a clean microscopic slide and a cover slide, and after a short thawing period and equilibration with room temperature (usually 5–10 min), the intensities of scattered light were measured as a function of scattering angle. Two experimental set-ups were used. One was a low angle He-Ne laser scattering apparatus operating at 632.8 nm. The scattered intensities as a function of angle were recorded on Kodak Plus X film (Eastman Kodak Co., Rochester, N.Y.). Photographic densities were converted to relative intensities by means of a densitometer (Photovolt Corp., New York). The other was a wide angle universal light scattering photometer (C. N. Wood Manufacturing Co. Newton, Pa.; model 3000) operating at 546 nm of the Hg lamp. The angular distribution of the scattered light intensities was obtained on a recorder. The low-angle apparatus provided an angular range from  $0.5$  to  $10^\circ$ , and the wide-angle apparatus from  $5$  to  $150^\circ$ . The time elapsed between sectioning and the completion of the measurements of the scattering intensities was between 10–15 min. Within this time domain no change in the scattering properties of the sections was observed.

Intensities were obtained both in the  $I_1(V_v)$  mode when the sample was between a polarizer and an analyzer that were aligned parallel to each other, and in the  $I_+(H_v)$  mode when the polarizer and analyzer were crossed. To be able to use thin sections that are cut under frozen conditions, preliminary experiments had to prove that the freezing and thawing processes do not alter the light-scattering properties of human lens sections. For that purpose, one lens was cut with a double-blade knife at room temperature into three sections, approximately 0.8 mm thick each. The lens sections were placed between a microscope slide and cover slide and the slides were sealed so that a constant thickness of the section was maintained. A 1-mm<sup>2</sup> portion of the section was illuminated, and the intensities of the scattered light were obtained as a function of scattering angle in both the low- and wide-angle apparatus. The illumination was centered on a spot of the section that did not give diffraction pattern. After obtaining the light-scattering intensities, the sections were frozen to  $-10$ ,  $-15$ , and  $-20^\circ\text{C}$  and kept there for 2–3 h. The sections were thawed out and equilibrated at room temperature. They were positioned in the apparatus so that approximately the same area was illuminated again. The intensity of the light-scattering patterns was obtained in both the wide- and low-angle apparatus. Fig. 2 shows the

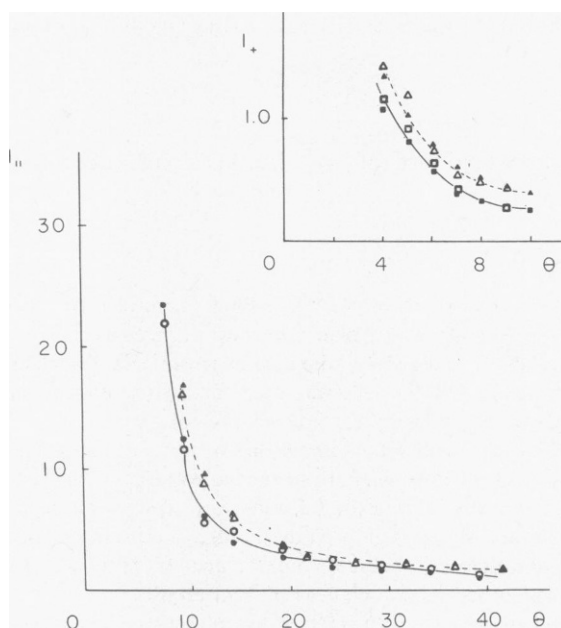


FIGURE 2 The effect of freezing and thawing on the light-scattering properties of two lens sections (1— and 2- - - - -) in the  $I_{||}$  and  $I_{\perp}$  mode. Symbols  $\circ$ ,  $\Delta$ ,  $\square$  before, and symbols  $\bullet$ ,  $\blacktriangle$ ,  $\blacksquare$  after the freezing-thawing cycle.

reproducibility of light-scattering intensities of two sections before and after freezing and thawing. It is evident while at wide angles, the reproducibility is excellent; at low angles, in both instruments, the reproducibility is less satisfactory. This is because the scattering at low angles is more intense than at higher angles and, therefore, the inability to position the sample "exactly" the same way before and after the freezing-thawing cycle affected the reproducibility at low angles to a greater extent. However, when the transmittance of the sample was measured before and after the freezing-thawing cycle, the reproducibility was  $\pm 0.5\%$ . Therefore, we may assume that the optical properties of the lens are not altered by a freezing-thawing cycle.

For the thin lens sections cut by microtome, the intensity of the scattered light as a function of the scattering angle for the range  $0.5\text{--}95^\circ$  was constructed by combining the data obtained in the low- and the wide-angle apparatus. Since these two experimental set-ups produce data that overlap in the range  $5\text{--}10^\circ$ , this range was used to calculate the conversion factor that expresses the low- and wide-angle results on the same scale. This procedure was adopted after it was shown that the product  $R(\theta)_{LA}\lambda_{LA}^4$  remains constant and equal to  $P(\theta)_{WA}\lambda_{WA}^4$  when different sections are compared in the region of overlap. On the basis of the experimental data a smooth curve (Debye and Bueche, 1949) was constructed.

The correlation functions  $\gamma(r)$  and  $f(r)$  were calculated from Eqs. 6 and 13 by performing the numerical integration with Simpson's rule. The experimental correlation functions were normalized by setting  $\gamma(0) = 1$  and  $f(0) = 1$ . The correlation lengths were calculated by a least-squares linear regression fitting of the experimental  $\gamma(r)$  and  $f(r)$  values to the forms given in Eqs. 9 and 14, respectively. Mean-squared average density and orientation fluctuations,  $\bar{\gamma}^2$  and  $\bar{\delta}^2$ , were calculated from Eqs. 5 and 11, respectively, by using the evaluated analytical forms of the correlation functions, Eqs. 9 and 14.

Fortran programs were written for these calculations, and a Burroughs B 6700 computer was used (Burroughs Corp., Detroit, Mich.).

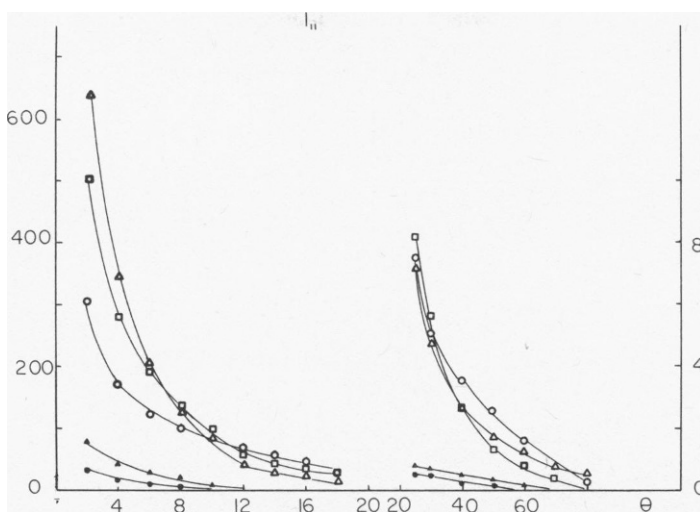


FIGURE 3 Light-scattering intensities in the  $I_1$  mode (in arbitrary units) of some human lens sections as a function of scattering angle ( $\theta$ ) and position of the section within the lens. ●—● 0.25 mm, ▲—▲ 0.435 mm, ○—○ 0.670 mm, □—□ 0.905 mm, △—△ 1.140 mm from the posterior lens surface.

## RESULTS

In Figs. 3 and 4, the primary light-scattering data are presented. The light-scattering intensities decrease monotonically with increasing scattering angle, in both  $I_1$  and  $I_+$  modes. In both modes, the scattering is independent of the azimuthal angle. The intensity of light scattering in the  $I_1$  mode is 20–50 times stronger than the  $I_+$ , at the same angle. It is also evident that as one progresses from the anterior or posterior surface of the lens inward, the intensity of scattered light increases in both the  $I_1$  and  $I_+$  modes.

The density correlation functions were obtained from the primary data. The experimental correlation function could be described well with the analytical function given in Eq. 9. Fig. 5 shows the fit between the experimental and calculated correlation function.

The correlation lengths of the density fluctuation are presented in Figs. 6 and 7. The first correlation length varies between 260 and 900 nm, and this correlation distance increases as one progresses from the cortical region of the lens toward the nucleus. The 59- and 82-yr-old lenses yielded similar first-correlation length distances, while the correlation lengths of the 31-yr-old lens were twice as high, although the transparency of the 31-yr-old lens was the highest. On the bases of the numerical values, and because this size is greater in the nucleus than in the cortex, one could assume that these distances represent the diameters of protein aggregates. Such aggregates have been shown in electronmicroscopic investigations to have diameters up to 500 nm (Kramps et al., 1975). In normal human lenses, such high molecular weight (HMW) protein aggregates are principally found in the nucleus (Spector et al., 1974).

The second correlation distance of the density fluctuation may represent the cytoplasmic medium in which the HMW protein aggregates are dispersed. This correlation distance (Fig.

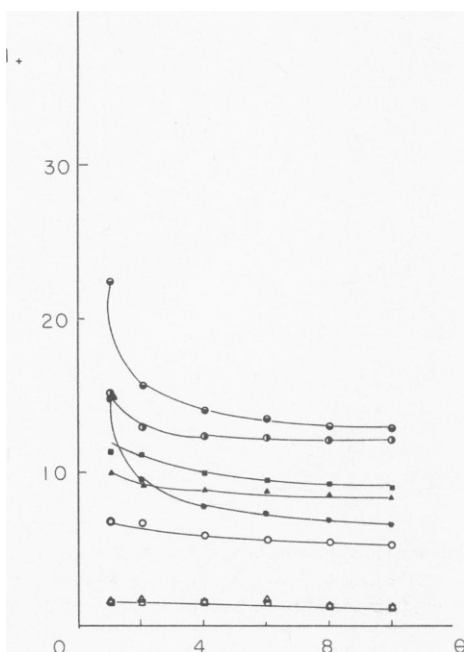


FIGURE 4

FIGURE 4 Light-scattering intensities in the  $I_+$  mode (in arbitrary units) of some human lens sections as a function of scattering angle ( $\theta$ ) and position of the section within the lens.  $\square$ — $\square$  0.250 mm,  $\bullet$ — $\bullet$  0.670 mm,  $\circ$ — $\circ$  0.905 mm,  $\circ$ — $\circ$  1.275 mm,  $\blacktriangle$ — $\blacktriangle$  1.410 mm from posterior lens surface and  $\square$ — $\square$  0.675 mm,  $\circ$ — $\circ$  0.590 mm,  $\triangle$ — $\triangle$  0.270 mm from the anterior lens surface.

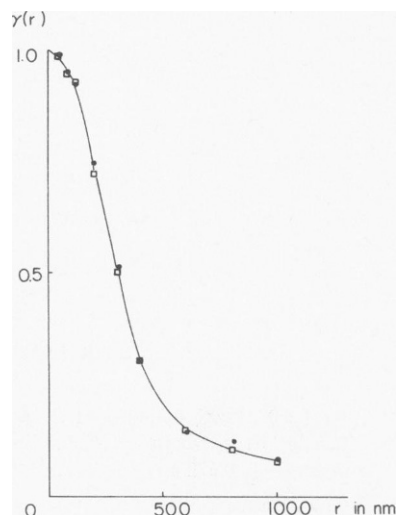


FIGURE 5

FIGURE 5 Experimental  $\square$ — $\square$  and calculated  $\bullet$ — $\bullet$  density correlation function  $\gamma(r)$  as a function of distance,  $r$ .

7) varies between 440 and 1,400 nm. On the basis of three lenses, no clear tendency can be established as to whether this distance is greater in the cortex or in the nucleus.

The amplitude of density fluctuation increases when one proceeds from the cortex to the nucleus. This is demonstrated in Fig. 8 by the plotting of the mean squared deviation from the mean refractive index against the position of the section within the lens. The magnitude of this mean squared deviation varies between  $2.5 \times 10^{-5}$  and  $8 \times 10^{-2}$ . The magnitude of the  $\bar{\eta}^2$  of the different lenses correlated well with the increase in light-scattering intensity, i.e., 59 > 82 > 31 yr old.

After the parameters of the density fluctuations were evaluated, the orientation correlation function was calculated. Because the  $I_1$  intensity is so much greater than  $I_+$ , the density correlation function  $\gamma(r)$  decreases faster than the Fourier transform of  $I_+$  (Eq. 13) with respect to  $r$ . This resulted in large uncertainties in the orientation correlation function,  $f(r)$ , at small  $r$  values. Therefore, we normalized the orientation correlation function by using values obtained at large  $r$  and extrapolated to small  $r$  values. Such a procedure implies that only approximate values of orientation correlation distances can be obtained and, therefore, the values given in Fig. 9 should be taken as indicating only the magnitude of these correlation distances. The orientation correlation distances  $b_1$  and  $b_2$  are of the same magnitude and vary between 600 and 2,600 nm.



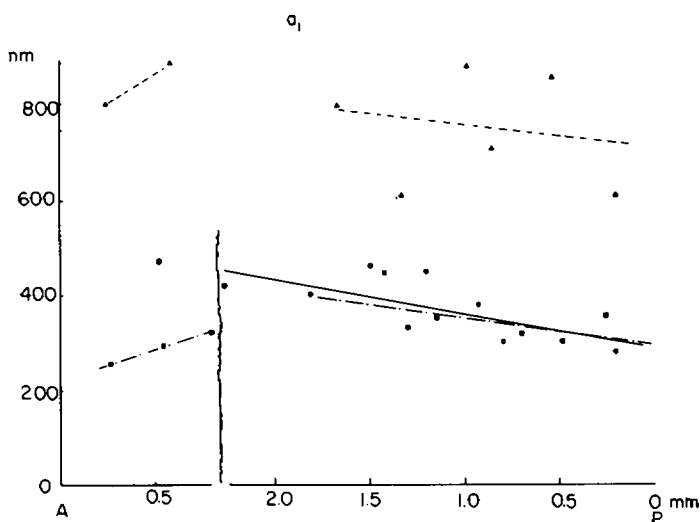


FIGURE 6 The first correlation distance,  $a_1$ , of density fluctuation (in nm) of lens sections as a function of position within the lens. (mm distance from anterior (A) and posterior (P) surface.)  $\triangle$ --- $\triangle$  31,  $\blacksquare$ --- $\blacksquare$  59, and  $\bullet$ --- $\bullet$  82-yr-old lens. The lines represent the least-square linear regression lines of the data presented. These notations apply to Figs. 6-11.

Because of the approximate nature of the orientation correlation function, the mean squared deviation from the mean refractive index in the orientation fluctuation will also have an approximate nature. The data presented in Fig. 10 varied between  $6 \times 10^{-8}$  and  $2 \times 10^{-6}$ .

## DISCUSSION

The main purpose of this article was to demonstrate that the theory of random fluctuations both in density and in orientation of optically anisotropic particles can be applied to light scattering of the human lens. The theory assumes that there is no cross correlation between

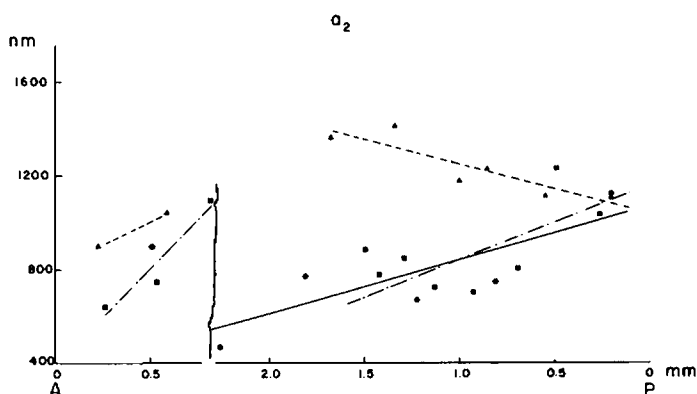


FIGURE 7 Second correlation distance,  $a_2$ , of density fluctuations in lens sections as a function of position within the lens.

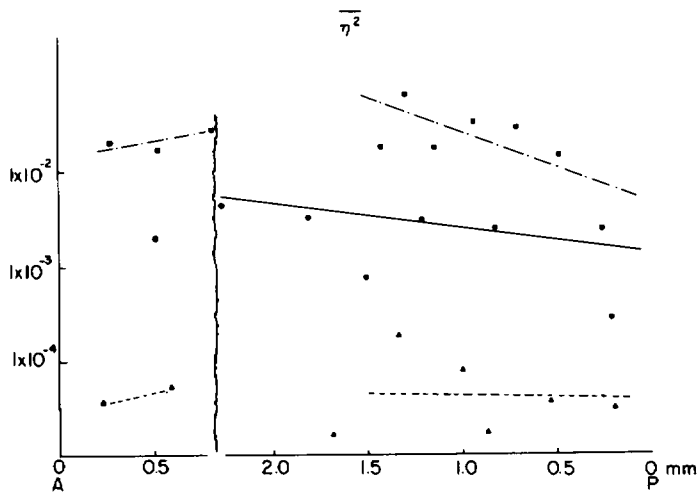


FIGURE 8 The mean squared deviations from the mean refractive index,  $\overline{\eta^2}$ , of density fluctuations in lens sections as a function of position within the lens.

the density and orientation fluctuation. This simplification enables an analytical solution; more refined theories would require a solution by computer simulation of the light-scattering patterns.

The fact that the light-scattering intensity decreases monotonically with increasing angle, and that there is no azimuthal angle dependence of scattering, implies that the theory of random fluctuation is applicable. This simple theory is applicable to thin lens sections only. In thick lens sections, or in the whole lens, an additional scattering occurs due to the regular spacings of cell membranes that give rise to simple or multiple diffraction patterns (Bettelheim and Vinciguerra, 1971; Bettelheim et al., 1973). The use of thin lens sections ( $\sim 10 \mu\text{m}$ ) reduces the diffraction effect, and the angular dependence of light-scattering

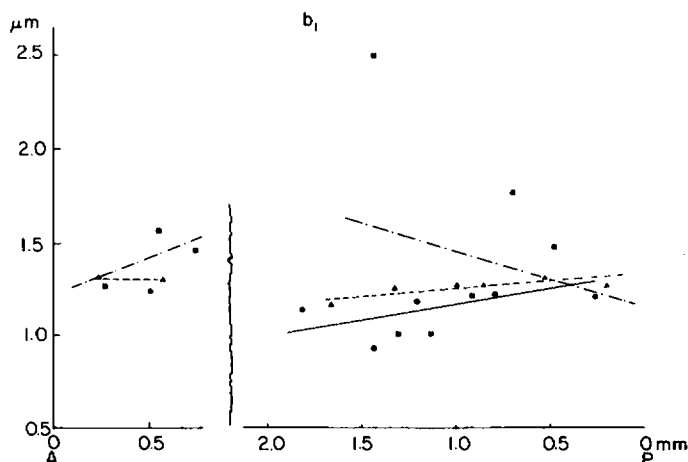


FIGURE 9 The first correlation distance,  $b_1$ , of orientation fluctuations (in  $\mu\text{m}$ ) of lens sections as a function of position within the lens.

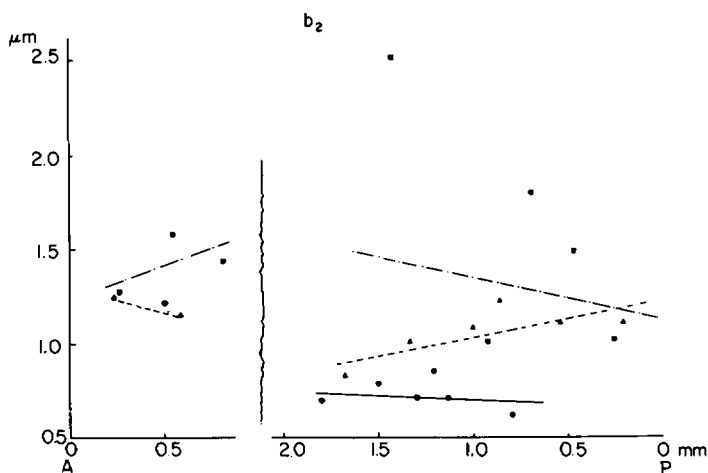


FIGURE 10 The second correlation distance,  $b_2$ , of orientation fluctuations of lens sections as a function of position within the lens.

intensity yields a smooth curve (Fig. 2). This means that the main contribution to the scattering comes from within the fiber cell, and this enables one to analyze the structures that cause light scattering.

The use of thin sections also reduces secondary and multiple scattering that would otherwise obscure the primary information obtainable from thin sections. In theory, one should use infinitely thin sections to eliminate the problem altogether. Otherwise, corrections must be applied to the experimental data (Stein and Keane, 1955). Hartel (1940) provided a theory that could be applied to different model systems such as spherulites (Prud'homme et al., 1974) or to rod-like morphology (Levesque and Prud'homme, 1977). In each case, one must obtain the turbidity as a function of thickness with the assumption that each successive infinitely thin layer in the actual sample will have the same scattering property. Such assumption for the lens of the eye is not valid, since there is a gradual increase in refractive index proceeding from the periphery of the cortex to the center.

Furthermore, the corrections are significant only when the turbidity of the sample is appreciable. For example, for the rod-like morphology, a 75% transmittance without correction introduces 10% error, and a transmittance of 50% without corrections causes a 22% error in the rod length calculated. In our case, the thin sections had 97–99% transmittance. Therefore, we came to the conclusion that the error in assuming uniformity in lens section would generate equal or greater error in the calculated parameters than would no correction at all. To be able to obtain thin sections, the lens must be frozen for sectioning. Our preliminary investigation on one normal human eye lens indicated that a freezing-thawing cycle does not alter the optical properties of the lens sections. Therefore, the adopted procedure to freeze the whole lens to  $-10^{\circ}\text{C}$  and section them from posterior to anterior normal to the visual axis provided sufficient samples (10 or more sections) to describe the topographic variation in scattering structures within the lens.

In a normal human eye the  $I_{\parallel}$  component of scattering is dominant (20–50 times stronger than the  $I_{\perp}$  component). This implies that the scattering in normal human eyes originates

mostly from density fluctuations. If density fluctuations alone are responsible for the scattering, no  $I_+$  component of the scattering would be observed. The fact that the intensity of the  $I_+$  component is weak and exists only at small angles makes the evaluation of the scattering parameters from orientation fluctuation somewhat uncertain. However, it has been demonstrated in galactose and xylose cataract formation in animal lenses (Bettelheim, 1978; Bettelheim and Bettelheim, 1978) and in a few human senile cataractous lenses (Bettelheim and Paunovic, 1978) that the  $I_+/I_{\parallel}$  ratio increases in cataract formation and can reach values as high as 0.4. The theory applied in this investigation yielded only approximate orientation fluctuations parameters, because we pushed the theory to its limit. However, the same theory, when applied to other lenses with higher  $I_+$  component of scattering and/or to cataract formation, can yield more accurate parameters of the orientation fluctuation. It must be emphasized also that the employment of thin sections is mandatory also in cataractous or high  $I_+$  scattering lenses. Multiple scattering produces depolarization and in itself may contribute to the  $I_+$  component.

Since most of the scattering originates from density fluctuations in normal human lenses, the size and amplitude parameters obtained from the theory can be scrutinized and compared to other measurements obtained in the literature.

By using the two-phase (dispersed and dispersant) model interpretations according to our analysis, we find that particles of the size of 200–900 nm are dispersed in media and separated from each other at 480–1400 nm distances. From human lenses (Jedziniak et al., 1973; Spector et al., 1974; Liem-The, 1975) HMW protein aggregates have been isolated by agarose gel chromatography that had molecular weight of  $15 \times 10^6$ – $3 \times 10^8$  and higher. These are the HMW aggregates of the water soluble proteins, and the water insoluble proteins are presumably even higher aggregates. If the proteins were compact spheres, a  $5 \times 10^7$ -dalton aggregate would have a diameter of 105 nm, and a  $5 \times 10^8$ -dalton aggregate a 310-nm diameter (Bettelheim, 1979). Liem-The (1975) has observed by electronmicroscopy that aggregates up to 500 nm appear in human lenses. Thus, our interpretation of our correlation distances as measuring the size of protein aggregates on the one hand, and their separation from each other, on the other, is supported by data in comparable literature.

The size of aggregates are larger in the nucleus than in the cortex. Previous literature reports that aggregation occurs primarily in the nucleus (Spector et al., 1971). The above considerations can explain the size parameters obtained from the 59- and 82-yr-old lenses. In these lenses, on the average, the aggregate sizes are smaller than the spacing between them. In the 31-yr-old lens, both correlation lengths  $a_1$  and  $a_2$  are larger than in the older lenses. That is, the fluctuation occurs over larger domains. The 31-yr-old lens scatters somewhat less light in spite of the larger correlation lengths because the amplitude of the fluctuation that is the refractive index difference between the domains is very small (Fig. 8), almost 100 times less than in the older lenses.

It is clear that the amplitude of the fluctuation is the most important contributor to the scattering in these three lenses. The differences in  $\bar{\eta}^2$  among the three lenses are of three magnitudes.

The amplitude of the refractive index fluctuation increases as one proceeds from either the anterior or posterior surface of the lens toward the center. A variation of  $\bar{\eta}^2$  from  $7 \times 10^{-3}$  to  $8 \times 10^{-2}$  implies a refractive index change from 0.06 in the cortex to 0.3 in the nucleus.

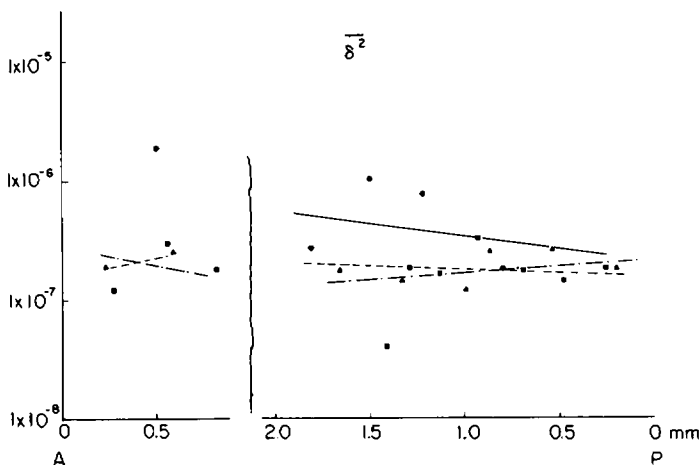


FIGURE 11 The mean squared deviations from the mean refractive index,  $\overline{\delta^2}$ , of orientation fluctuations in lens sections as a function of position within the lens.

Philipson (1969) has shown that the mean refractive index of rat lens increases from periphery to center. In old rats, this increase in mean refractive index increases from 1.38 in the cortex to 1.50 in the nucleus. A similar trend was reported (Philipson, 1973) in human lenses. Thus, the range and the trend of the refractive index fluctuation amplitude obtained from our light scattering measurement agrees with data obtained by other means.

Regarding the parameters of the optical anisotropy fluctuations, we can discuss only the magnitude of the numerical values because of the approximations used in obtaining the correlation functions. Anisotropic structures of the dimension of 1–2  $\mu\text{m}$  and longer have been observed as cytoplasmic filaments of about 10–14 nm in diameter (Lasser and Balazs, 1972; Maisel, 1977; Rafferty and Goossens, 1978). Whether such geometrically anisotropic structures are also optically anisotropic remains to be proven. However, the hypothesis that the form birefringence of the fiber cell is balanced with intrinsic birefringence (Bettelheim, 1975) requires that such optically anisotropic structures should be present in the fiber cells.

Finally, the magnitude of the optical anisotropy fluctuations are very small. The deviations from the mean,  $\overline{\delta^2}$ , are  $10^3$ – $10^5$  smaller than the deviations from the mean in the density fluctuations (Fig. 11). This would explain why the  $I_+$  component of the scattering is so weak in spite of the fact that the dimensions of the particles contributing to the orientation fluctuations are almost 10 times larger than those contributing to the density fluctuations.

In conclusion, the application of the theory of random fluctuations in density as well as in optical anisotropy describes well the structural components that contribute to the light scattering of human lens. In subsequent articles, we shall describe the variations of the light scattering parameters in individual normal eyes as a function of aging, and will apply the same considerations to cataractous lenses of different etiology.

We would like to thank Dr. Stephen Goldberg of Adelphi University for the use of some of his computer programs. We also thank the New York Eye Bank for the donated lenses.

## REFERENCES

- ALEXANDER, L. E. 1969. X-ray Diffraction Methods in Polymer Science. John Wiley & Sons, Inc. New York. 296.
- BENEDEK, G. B. 1971. Theory of transparency of the eye. *Appl. Opt.* **10**:459.
- BETTELHEIM, F. A. 1975. On the optical anisotropy of lens fiber cells. *Exp. Eye Res.* **21**:231.
- BETTELHEIM, F. A. 1978. Induced optical anisotropy fluctuation in the lens of the eye. *J. Colloid Interface Sci.* **63**:251.
- BETTELHEIM, F. A. 1979. Syneresis and its possible role in cataractogenesis. *Exp. Eye Res.* In press.
- BETTELHEIM, F. A., and A. A. BETTELHEIM. 1978. Small angle light scattering studies on xylose cataract formation in bovine lenses. *Invest. Ophthalmol. Visual Sci.* **17**:896.
- BETTELHEIM, F. A., and M. PAUNOVIC. 1978. Light scattering parameters of human cataracts. *Abstr. Third Int. Cong. Eye Res.* Osaka, Japan. 111.
- BETTELHEIM, F. A., and M. J. VINCIGUERRA. 1971. Laser diffraction patterns of highly ordered superstructures in the lenses of bovine eyes. *Ann. N.Y. Acad. Sci.* **172**:429.
- BETTELHEIM, F. A., M. J. VINCIGUERRA, and D. KAPLAN. 1973. Dynamic laser diffraction of bovine lenses. *Exp. Eye Res.* **15**:149.
- DEBYE, P., and A. M. BUECHE. 1949. Scattering by an inhomogeneous solid. *J. Appl. Physiol.* **20**:518.
- GALLAGHER, L., and F. A. BETTELHEIM. 1962. Light scattering studies of cross-linking unsaturated polyesters with methyl acrylate. *J. Polym. Sci.* **58**:697.
- HARTEL, W. 1940. Zur Theorie der Lichtstreuung durch trübe Schichten, besonders Trütbläser. *Licht.* **10**:141.
- JEDZINIAK, J. A., J. H. KINOSHITA, E. M. YATES, L. O. HOCKER, and G. B. BENEDEK. 1973. On the presence and mechanism of formation of heavy molecular weight aggregates in normal and cataractous human lens. *Exp. Eye Res.* **15**:185.
- KAHOVEC, L., G. POROD, and H. RUCK. 1953. X-ray small-angle investigations on closepacked colloid systems. *Kolloid Z.* **133**:16.
- KRATKY, O. 1966. Possibilities of X-ray small-angle analysis in the investigation of dissolved and solid high-polymer substances. *Pure Appl. Chem.* **12**:483.
- KRAMPS, H. A., A. L. H. STOLS, H. J. HOENDERS, and K. DEGROOT. 1975. On the quaternary structure of high molecular weight proteins from the bovine eye lens. *Eur. J. Biochem.* **50**:503.
- LASSER, A., and E. J. BALAZS. 1972. Biochemical and fine structure studies on the water insoluble components of the calf lens. *Exp. Eye Res.* **13**:292.
- LEVESQUE, D., and R. E. PRUD'HOMME. 1977. Small angle light scattering from thin polymer films: multiple scattering from samples with rod like morphology. *J. Polym. Sci. Part A-2.* **15**:1613.
- LIEM-THE, K. N. 1975. The structural proteins of the rabbit eye lens after X-ray irradiation. Ph.D. Thesis. University of Nijmegen, the Netherlands.
- MAISEL, H. 1977. The effect of urea on the lens intra-cellular matrix and soluble lens protein. *Exp. Eye Res.* **25**:595.
- MAISEL, H., and M. M. PERRY. 1972. Electron microscope observations on some structural proteins of the chick lens. *Exp. Eye Res.* **14**:7.
- PERRY, M. M. 1976. A method to demonstrate the fine structural components of lens fiber cells. *Exp. Eye Res.* **22**:125.
- PHILIPSON, B. 1969. Distribution of protein within the normal rat lens. *Invest. Ophthalmol.* **8**:258.
- PHILIPSON, B. 1973. Changes in the lens related to the reduction of transparency. *Exp. Eye Res.* **16**:29.
- PRUD'HOMME, R. E., L. BOURLAND, R. T. NATARAJAN, and R. S. STEIN. 1974. Scattering of light from thin polymer films. I. Multiple scattering. *J. Polym. Sci. Part A-2.* **12**:1955.
- RAFFERTY, N. S., and E. A. ESSON. 1974. An electron-microscope study of adult mouse lens: some ultrastructural specialization. *J. Ultrastruct. Res.* **46**:239.
- RAFFERTY, N. S., and W. GOOSSENS. 1978. Cytoplasmic filaments in the crystalline lens of various species: functional correlation. *Exp. Eye Res.* **26**:177.
- SPECTOR, A., T. FREUND, L. K. LI, and R. C. AUGUSTEYN. 1971. Age dependent changes in the structure of alpha crystallin. *Invest. Ophthalmol.* **10**:677.
- SPECTOR, A., L. K. LI, and J. SIGELMAN. 1974. Age dependent changes in the molecular size of human lens proteins and their relationship to light scatter. *Invest. Ophthalmol.* **13**:795.

- STEIN, R. S. 1969. The determination of the inhomogeneity of crosslinking of a rubber by light scattering. *Polym. Lett.* **1**:657.
- STEIN, R. S., and J. J. KEANE. 1955. The scattering of light from thin polymer films. I. Experimental procedure. *J. Polym. Sci.* **17**:21.
- STEIN, R. S., J. J. KEANE, F. H. NORRIS, F. A. BETTELHEIM, and P. R. WILSON. 1959. Some light scattering studies of the texture of crystalline polymers. *Ann. N. Y. Acad. Sci.* **83**:37.
- TROKEL, S. 1962. The physical basis for transparency of crystalline lens. *Invest. Ophthalmol.* **1**:493.
- WANKO, T., and M. A. GAVIN. 1959. Electronmicroscope study of lens fibers. *J. Biophys. Biochem. Cytol.* **6**:67.
- WUN, K. L., and W. PRINS. 1974. Assessment of non-random crosslinking in polymer networks by small angle light scattering. *J. Polym. Sci. Part A-2.* **12**:533.